Applied Surface Science 348 (2015) 85–91

Contents lists available at ScienceDirect

Applied Surface Science

journal homepage: www.elsevier.com/locate/apsusc

# In liquid laser treated graphene oxide for dye removal

Paola Russo[a,b,*], Luisa D'Urso[a], Anming Hu[c], Norman Zhou[b], Giuseppe Compagnini[a]

[a] Dipartimento di Scienze Chimiche, Universita' degli Studi di Catania, Viale Andrea Doria 6, Catania 95125, Italy
[b] Department of Mechanical and Mechatronics Engineering, University of Waterloo, 200 University Ave., West Waterloo, Ontario N2L 3G1, Canada
[c] Department of Mechanical, Aerospace and Biomedical Engineering, University of Tennessee, Knoxville, TN 57996-2210, USA

ARTICLE INFO

*Article history:*
Received 7 August 2014
Received in revised form
12 November 2014
Accepted 3 December 2014
Available online 10 December 2014

*Keywords:*
Graphene oxide
Reduced graphene oxide
Adsorption
Methylene blue

ABSTRACT

The presence of dyes, pharmaceuticals and many other pollutants in wastewaters is critical due to severe effects on the human beings and on the environment. Here, solutions of graphene oxide (GO) and reduced graphene oxide (rGO) were tested as adsorbents for the removal of methylene blue (MB), a cationic dye, from aqueous media. The reduced forms of graphene oxide were obtained after laser irradiation of colloidal suspensions of graphene oxide, obtained by the Hummers and Offeman's method. We observed that both graphene oxide and its reduced forms are excellent adsorbents towards methylene blue. In particular, rGO showed a higher adsorption capacity than GO, suggesting that a strict control of laser irradiation time permits to obtain rGO with different degrees of reduction and therefore the residual oxygenated functional groups may influence the adsorption behaviour more or less. Characterization of the samples by atomic force microscopy (AFM) showed that produced rGO sheets via laser irradiation exhibited a discontinuous surface where some holes could be detected contributing to an enhancement of the rGO surface area that is a higher adsorption capacity.



## 1. Introduction

Water treatments for the elimination of contaminants such as pesticides, pharmaceuticals, personal care products (PPCPs) and dyes are currently in the centre of many studies [1–3]. In particular, the coloured wastewaters of textile industries, which employ dyes and pigments to colour their product, represent serious problem to the environment [4]. Dyes are toxic, non-biodegradable, undergo to chemical changes and consume dissolved oxygen from rivers. Thus, these substances are harmful to aquatic organisms and to humans as well. For example, intense exposure to methylene blue dye may cause eye burns, vomiting, mental confusion and so on [5]. Therefore, dyes removal from wastewaters is of vital importance.

Across the years, a large number of physical, chemical and biological processes have been developed in order to remove these contaminants from wastewaters. These methods include adsorption [6,7], precipitation [8], coagulation [9], oxidation processes [10], photocatalysis [11–13], etc. Among these, adsorption processes onto suitable adsorbents have been widely employed for the removal of coloured pollutants from textiles, papers and cosmetics industries wastewaters [14–17]. Generally, activated carbons are employed as adsorbents for dyes removal due to their elevated surface areas [3,18,19]. However, activated carbons derive from natural materials such as wood or coal making their production and regeneration quiet expensive [20]. Therefore, many researchers studied alternative ways for the production of low-cost adsorbents. Among non-carbonaceous adsorbent there are $TiO_2$ nanowires [12], zinc ferrite nanoparticles [21] or mesoporous $Cu_2O$ submicro-spheres [22]. However, the presence of metallic elements increases the cost. Consequently, carbon-based materials due to their properties such as low-cost, chemical stability, structural diversity have attracted more attention. This led many researchers to exploit novel carbon-based materials, for instance, low-cost activated carbon were obtained from agriculture by-products such as palm-tree cobs, rattan sawdust or rice husks. Recently, graphene and graphene oxide are drawing much attention as alternative materials for adsorption [23–26]. Graphene is defined as a flat monolayer of $sp^2$ carbon atoms, packed tightly into a two-dimensional (2D) honeycomb lattice [27]. Besides, graphene oxide is obtained from the oxidation of graphene and it contains a huge number of functional groups such as hydroxyl, carboxyl and epoxy groups. Since graphene discovery in 2004, it has attracted the interest of many scientists due to its outstanding electrical, mechanical and thermal properties. Moreover, graphene and graphene oxide due to their large theoretical surface area (as high as 2630 $m^2/g$) [28] and the presence of the oxygen groups which are responsible for the formation of stable aqueous colloid are promising materials to

* Corresponding author at: Department of Mechanical and Mechatronics Engineering, University of Waterloo, 200 University Ave, West Waterloo, Ontario N2L 3G1, Canada. Tel.: +1 (519) 888 4567x35625.
*E-mail address:* rsspla1@gmail.com (P. Russo).

http://dx.doi.org/10.1016/j.apsusc.2014.12.014
0169-4332/

adsorbs various substances such as dyes, heavy metals and phenols [29]. One of the advantages of graphene oxide as adsorbent is that it has a very high negative charge density due to the presence of these oxygenated functional groups. Therefore, graphene oxide can interact with positively charged species such as metal ions, polymers and cationic dyes [24]. It has been reported that graphene oxide and reduced graphene oxide can be considered as promising adsorbent of methylene blue (MB) dye. It was stated that the adsorption mechanism could be ascribed either to the electrostatic attraction between them or to the π–π interactions between aromatic materials and graphene. For this reason, the strict control of the degree of reduction is crucial. This implies the capability of tuning the density and quality of the functional groups, which separate the $sp^2$ domains on the graphene platform. Recently, we have reported the reduction of grapheme oxide sheets by the pulsed laser ablation in liquid (PLAL) technique [30]. Generally, PLAL is a powerful technique, which permits the synthesis of nanoparticles and fabrication of nanostructures in the colloidal state as extensively reported by many authors [31–33]. One of the advantages of the PLAL over the common methods for the grapheme reduction [34–37] is the absence of byproduct formation during the synthesis [31] that makes this method greener than other approaches [30]. In this paper, pulsed laser irradiation is used to gradually reduce solutions of chemically prepared GO and the resulting samples have been tested as adsorbents for MB removal in aqueous media.

## 2. Experimental

### 2.1. Materials

Natural Graphite flakes were purchased from Aldrich. Potassium permanganate, sodium nitrate were purchased form VWR Chemicals, sulfuric acid was purchased from AnalaR Normapur. Hydrogen peroxide and Methylene blue were purchased from Sigma–Aldrich.

### 2.2. Preparation of the adsorbents

#### 2.2.1. Synthesis of graphene oxide (GO) and reduced graphene oxide (rGO)

GO was prepared by a modified Hummers and Offeman's method, as previously reported [30]. AFM analysis showed that the GO sheets obtained had a thickness of ~0.7 nm (see figure S1 in SI), which is in agreement with the values reported in literature for graphene oxide dispersions in water [38,39]. The GO layers are thicker than single-layer graphene sheets (0.34 nm) due to the presence of the oxygen-containing functional groups within the basal plane and to the roughness attributed to $sp^3$ centres and point defects in the carbon lattice.

The reduction of GO oxide was performed following the method reported in our previous work [30]. Briefly, different solutions of GO were irradiated by the second harmonic of a pulsed Nd:YAG laser with a pulse duration of 5 ns a repetition rate of 10 Hz. The laser beam size was around 28 $mm^2$ and the GO solutions were homogeneously irradiated, without any focusing lens, at a constant fluence of 0.32 $J/cm^2$ for different time. In such a way, we obtained stable solutions of rGO with different degree of reduction and several characterization analysis confirmed the occurred reduction. We hypothesized that the reduction of the GO sheets exposed to laser irradiation occurs, because the GO sheets undergo to a mechanism similar to the solvothermal reduction of graphene oxide [34–37].

For the adsorption experiments, we employed two solutions of rGO: rGO-30 and rGO-90 obtained after 30 and 90 min of laser irradiation, respectively.

#### 2.2.2. Adsorption experiments

The adsorption abilities of GO, rGO-30 and rGO-90 were measured employing methylene blue (MB) dye as adsorbate. The dye adsorption experiments were carried out in a 50 ml glass container under agitation. 3 ml of 0.17 mg/ml GO (rGO-30, rGO-90) was put into 30 ml of dye solution with an initial concentration of 12 mg/l (pH 6, 298 K). At regular intervals of time, aliquots of solution (3 ml) were taken from the solution and the concentration of the residual MB was determined using a UV–Vis spectrophotometer by monitoring the absorbance at 664 nm. The amount of MB adsorbed at time $t$, $q_t$ (mg/g), was calculated according to Eq. (1):

$$q_t = \frac{[(C_0 - C_t)V]}{m} \quad (1)$$

where $C_0$ is the initial concentration of MB (mg/l), $C_t$ is the amount of adsorbed MB on the adsorbent (mg/g), $V$ is the volume of the solution (l) and $m$ is the mass of adsorbent (g).

### 2.3. Characterization of the samples

The reduction of GO sheets and the residual concentration of MB were monitored with a UV–Vis Perkin Elmer lambda 2 Spectrometer in the range 190–900 nm.

Zeta potentials of GO and rGO solutions were measured by using a Horiba Scientific NanoParticle Analyzer SZ-100-Z. XPS analysis was carried out in order to verify the reduction of GO sheets by laser irradiation. Some drops of GO and rGO solutions were deposited onto silicon wafers and the XPS analyses were performed using a PHI ESCA/SAM 5600 Multy technique spectrometer equipped with a monochromatized AlKa X-ray source operating at 250 W at a base pressure of 10–10 mbar. Raman scattering has been excited by the 514.5 nm radiation of an Ar ion laser and analyzed by a Jobin Yvon 450 mm focal length monochromator, equipped with a CCD camera detector cooled at 77 K. The incident laser beam was focused by a 100× objective and the laser power on the samples was kept to a minimum to avoid heating. The surface morphology of GO and rGO samples was investigated by Atomic Force Microscopy (NT-MTD AFM) performed operating in the tapping mode and using a $SiO_2$/Si substrate.

## 3. Results and discussion

In Fig. 1a, we report the UV–Vis spectra of the as prepared GO solution and the GO solution irradiated for 30 min and 90 min, labelled as rGO-30 and rGO-90, respectively.

As previously reported [30], laser irradiation of GO led to a decrease of the absorption at 300 nm, which suggested that the concentration of C=O groups is decreasing upon laser irradiation. Moreover, this effect is correlated to a red shift of the signal relative to the $\pi$–$\pi^*$ transitions meaning a restoring of the $sp^2$ hybridization. The laser reduction of the GO solutions was further confirmed by a decrease of the energy gap. In particular, we found that the band gap decreased from 2 eV (GO) to ~1.25 eV (rGO-90) upon laser irradiation, as shown in Fig. 1b. Bandgap values have been obtained using the well-known Tauc's expression [40,41], in which the optical band gap ($E_g$) is obtained as follows:

$$(\alpha E)^{1/2} = [A(E - Eg)]^{1/2} \quad (2)$$

where $\alpha$ is proportional to the absorbance and $A$ is a constant. The band gap depends on the size, shape, and fraction of the $sp^2$ domains, in particular the energy gap decreases gradually as the size of graphitic domains increases [42].

Chemical analyses performed by XPS confirm this view as reported in figure S2 (S.I.). A decrease of the oxygen-containing groups (C—OH, C—O, C=O and COOH) and an increase of carbon $sp^2$ (C=C) in the basal plane can be noted after the laser irradiation of

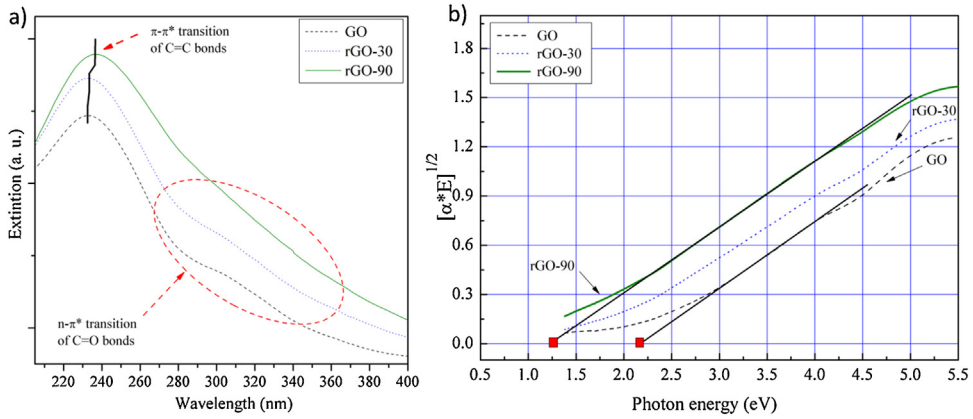


**Fig. 1.** (a) UV–Vis absorption of GO (black dashed line) and GO after 30 (blue dotted line) and 90 (green solid spectrum) minutes of laser irradiation; (b) decrease of the GO energy gap upon laser reduction. (For interpretation of the references to color in this figure legend, the reader is referred to the web version of this article.)

GO. These results are in accordance with the previously mentioned decrease of the energy gap. In rGO sample the C—OH and C—O peaks are accounted for 17,7% and 24.1%, respectively, instead of 23.4% and 35.9% in the case of the as prepared GO sample. The C=C peak in rGO accounted for 44.4% instead of 25.1% in the as-prepared GO, proving the GO reduction.

The reduction of GO was further confirmed by Raman spectroscopy, which is a powerful technique employed for the structural characterization of graphitic materials [43]. The main Raman features of carbon materials are the G band around 1600 $cm^{-1}$ which originates from in-plane vibration of $sp^2$ carbon atoms and the D band at around 1350 $cm^{-1}$ arising from a defect-induced breathing mode of $sp^2$ rings. It has been reported that the reduction of graphene oxide can be investigated from the value of the intensity ratio ($I_D/I_G$) [44]. In particular, as reported by Sobon [44] since the intensity of the D band is related to the size of $sp^2$ domains, an increase of its intensity can be correlated to an increase of $sp^2$ domains. Therefore, reduced graphene oxide should possess a higher ($I_D/I_G$) intensity ratio than graphene oxide. The Raman spectra of our samples, with the relative ($I_D/I_G$) intensity ratios, are shown in figure S3. It is possible to note that the as prepared GO had an ($I_D/I_G$) intensity ratio of 0.85 which increased up to 0.94 after laser irradiation, confirming that the reduction successfully occurred.

One of the most important properties of GO suspension is the stability of the system towards clustering and precipitation. This is much more important if these systems are considered for the removal of contaminants in wastewaters. Actually, the stability of the solutions is strongly correlated to the effective surface charge associated with the double layer around the GO sheets. This was studied by zeta potential measurements, before and after the laser irradiation, considering that stable solutions of GO shows a zeta potential more positive than +30 mV or more negative than −30 mV [45]. The results of zeta-potential measurements are shown in Fig. 2. GO prepared by the modified Hummers method has a zeta-potential of −63 mV resulting quite stable in aqueous solution. This is a consequence of the negative charge due to the ionization of the carboxyl and phenol groups existing on the surface of GO sheets [46]. After laser irradiation, we observed a decrease, unless the sign, of the zeta-potential. In particular, rGO-30 showed a ζ-potential of −56 mV, while the one relative to rGO-90 was −50 mV because of the removal of oxygenated functional groups. Although these ζ-potential values are lower than the one of as-prepared GO, they result stable since, as aforementioned, ζ-potential values more negative than −30 mV are generally considered to represent sufficient mutual repulsion to ensure the stability of a dispersion. Further results have shown that the parameters of the saturation curve reported in Fig. 2 are correlated with the irradiation parameters in terms of wavelength and laser fluence. A change in these values generally produces different saturation values as well as different time constant in an experimental-like kinetic law reported. The laser fluence is then a key parameter for GO reduction and an accurate control of it permits to obtain rGO solutions with different degrees of reduction.

To our knowledge, adsorption studies of methylene blue on graphene oxide and reduced graphene oxide have been always performed using hydrazine as a reduction agent. We have studied the efficiency of GO and its laser reduced forms for the adsorption of MB in water. A detailed description of the adsorption experiments has been reported in the previous section.

Experimentally, we found that when GO and rGO were added to the MB solution, the mixture became unstable and immediately an aggregation phenomenon occurred. At regular intervals of time, aliquots of the mixed solution were taken and the concentration of the residual MB was determined using a UV–Vis spectrophotometer and the spectra obtained are reported in Fig. 3. It can be seen that, in accordance with the aggregation phenomenon we detected, when GO (rGO) is added to the solution the concentration of the residual MB rapidly drop down and after 40 min an equilibrium is reached.

The amount of MB adsorbed ($q_t$) at time $t$, was calculated according to Eq. (1) and is reported in Fig. 4 for GO, rGO-30 and rGO-90.

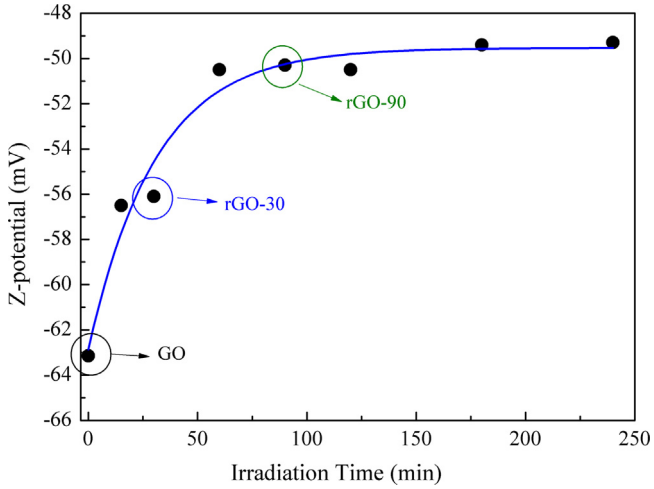


**Fig. 2.** Zeta-potential of GO and rGO solutions at increasing irradiation time. The curve represents a fit with exponential law.

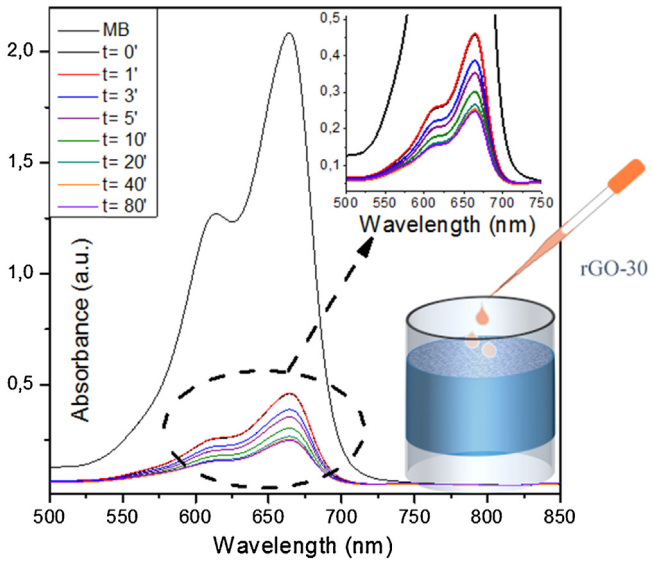


**Fig. 3.** UV–Vis spectra of residual MB after the addition of 3 ml of rGO-30.

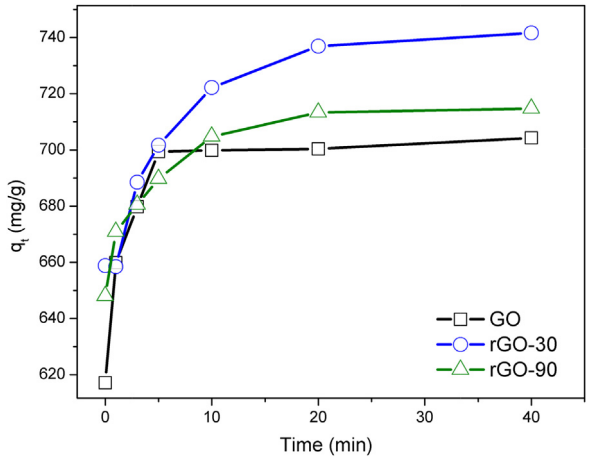


**Fig. 4.** Adsorption of MB on graphene oxide and its reduced forms as a function of time.

Noteworthy, the adsorption of MB is initially very fast and in a few seconds, $q_t$ reaches values of around 600 mg/g. This fast stage was followed by a slower adsorption stage lasting for about 3 min and then, after 20 min, the adsorption capacity reaches the equilibrium. The fast adsorption stage is attributed to the adsorption of MB dyes on the external surface of the adsorbents. This behaviour might be ascribed to the fact that GO and rGO possess a highly negative surface charge, which favours the adsorption of cationic molecules, such as the MB dye, on their surfaces through electrostatic attraction [47]. Conversely, the slower adsorption process can be related to the intra-particle diffusion, suggesting that adsorption mechanism is quite complex and involves different steps [48]. To understand better the adsorption mechanism, adsorption kinetics was investigated. The adsorption process can be described with several mathematical models, which can be classified as adsorption reaction models and adsorption diffusion models [48]. To describe the adsorption mechanism, the kinetic profiles were evaluated with the pseudo-first order, pseudo-second order and intra-particle diffusion reaction models.

The pseudo-first order rate equation is given by Eq. (3):

$$\ln(q_e - q_t) = \ln q_e - k_{1t} \tag{3}$$

where $q_e$ and $q_t$ are the amounts of adsorbed MB on the adsorbent (mg/g) at equilibrium and at time $t$, respectively, and $k_1$ is the pseudo-first order rate constant ($min^{-1}$). The pseudo-first order rate constant $k_1$ was calculated from the slope of the plot of $\ln(q_e - q_t)$ versus $t$. The kinetic parameters and the correlation coefficients ($R^2$) were determined by linear regression. However, the data did not fit well and that $R^2$ values were low, as shown in Table S1 (Supporting Information). This shows that the MB adsorption on graphene oxide and on its reduced form did not follow the pseudo-first order kinetic model, as observed also by other groups working on the adsorption of MB on graphene oxides [28,47,49].

The pseudo-second order kinetic model assumes that the rate limiting step involves chemisorption of adsorbate on the adsorbent. The pseudo-second-order rate equation is given by Eq. (4):

$$\frac{t}{q_t} = \left[\frac{1}{k_2(q_e)^2} + \left(\frac{1}{q_e}\right)t\right] \tag{4}$$

where $k_2$ is the adsorption rate constant ($g\,mg^{-1}\,min^{-1}$), $q_e$ and $q_t$ are the amounts of adsorbed MB on the adsorbent (mg/g) at equilibrium and at time $t$, respectively. The values of $t/q_t$ as function of time was calculated for each material and by fitting the data, the adsorption rate constant and the value of $q_e$ for each adsorbent were obtained and summarized in Table 1.

The pseudo-second order kinetic model is more suitable for describing the adsorption kinetics compared with the pseudo-first order one. The $R^2$ correlation coefficient is 1 for all the adsorbents and the calculated values of equilibrium capacity, $q_e$, agree well with experimentally measured capacity. The pseudo-second order kinetics fitted plots of the adsorption of MB are reported in figure S4. It is possible to note that, GO and rGO-90 can uptake up to 700 mg/g of MB while for rGO-30 the adsorption capacity slightly increased up to 746 mg/g. Moreover, rGO showed lower rate constants than as prepared GO, suggesting that the adsorption mechanism might be different. We believe that this difference is ascribed to a change in the structure of the GO sheets upon laser irradiation, and for this reason we have investigate the morphology of GO and rGO samples by AFM (Fig. 5b and c), thus observing that the surface of the rGO sheets start to appear like a porous network.

The pores resulted to be around ~50–20 nm wide either for rGO-30 or for rGO-90 and we assumed that the increase of the roughness could be ascribed to the formation of this porous structure. Further irradiation (more than 90 min) leads to a fragmentation of the porous network and probably this is the beginning of a process which leads to the formation of GO nanodots [50]. Consequently, the increase of the adsorption capacity for rGO-30 could be related to the presence of macro and mesopores, which enhanced the adsorption process, while the decrease of the adsorption capacity at 90 min or above can be ascribed to the aforementioned fragmentation of the sheets, which lead to a drop of the adsorption sites. Preliminary results have demonstrated that this decrease continues for higher irradiation times.

The pseudo-first and pseudo second order models cannot give information or evaluate the contribution of intra-particle diffusion to the adsorption mechanism.

In general, adsorption process in porous media is governed by three steps:

(1) Instantaneous adsorption step.
(2) Gradual adsorption step where the dye molecules move within the pores of the adsorbents and where the intra-particle diffusion is the rate-limiting mechanism.
(3) The final equilibrium step where the dye moves slowly from mesopores to micro pores causing a slow adsorption step [51].

**Table 1**
Pseudo-second order kinetic for adsorption of MB on GO and laser treated GO and intra-particle diffusion model parameters obtained for GO and rGO.

| Adsorbents | [MB] (mg/L) | Pseudo-second order model | | | Intra-particle diffusion model | | | |
|---|---|---|---|---|---|---|---|---|
| | | $q_{e,calc}$ (mg/g) | $K_2$ (g/mg min) | $R^2$ | $k_{p1}$ (mg/g min$^{0.5}$) | $R^2$ | $k_{p2}$ (g/mg min$^{0.5}$) | $R^2$ |
| GO | 12 | 704 | 0.017 | 1 | 1.16384 | 0.93474 | // | // |
| rGO-30 | 12 | 746 | 5.37E−3 | 0.99999 | 17.4197 | 0.9818 | 1.8677 | 0.9872 |
| rGO-90 | 12 | 719 | 9.66E−3 | 0.99999 | 11.8445 | 0.9728 | 0.4636 | 0.9634 |

From this point of view, kinetic results have been analyzed using the so called "intra-particle diffusion" model proposed by Weber and Morris [1,52].

The intra-particle diffusion model is described using the Eq. (5):

$$q_t = k_p t^{0.5} + C \quad (5)$$

where $C$ is the intercept and $k_p$ is the intra-particle diffusion rate constant (mg/g min$^{-1/2}$). According to this model if the intra-particle diffusion controls the adsorption kinetics, the plot of $q_t$ versus $t^{0.5}$ should give a straight line passing through the origin. However, if multi-linearity is observed, this means that different mechanisms with different rate constants are involved in the adsorption and multiple linear regressions must be applied for each linear region [19].

In Fig. 6, are displayed the plots obtained for the three material tested. The plots obtained for rGO-30 and rGO-90 are comprised of three linear regions revealing that different mechanism are involved in the adsorption mechanism. The first linear part (0–2 min, not shown) can be correlated to an external surface adsorption or instantaneous adsorption followed by two linear sections representing the intra-particle diffusion, where the dye moves within the pores of the adsorbent. The intra-particle diffusion parameters, $k_{p1}$ and $k_{p2}$, for these regions were determined from the slope of the plots and are reported in Table 1. The rate parameter for the diffusion in the two regions is attributed to one type of pore (macro) diffusion labelled as $k_{p1}$ and to another pore (meso) diffusion labelled as $k_{p2}$ [52], confirming the presence of pores of different diameters within the plane of rGO sheets. Noteworthy, the rate parameter $k_{p1}$ is higher than $k_{p2}$ either for rGO-30 or for rGO-90. This is due to the relative free path for diffusion available in each type of pore size. As the pore dimensions decrease, the free path becomes less, with possible pore blockage occurring with a dramatic reduction in the diffusion parameters [52].

For GO (the first linear region (0–3 min) is not reported) the plot obtained showed a straight line not passing through the origin, revealing that the adsorption in GO is dominated by the mass

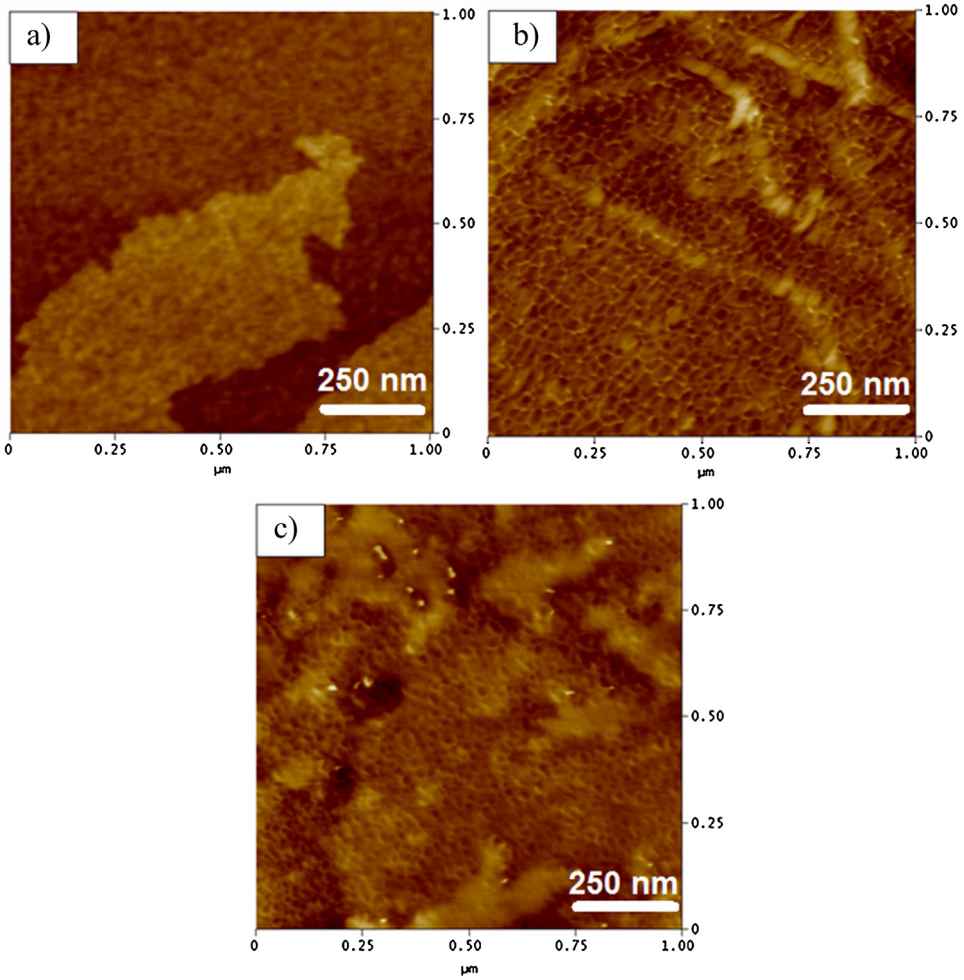


**Fig. 5.** (a) AFM image of GO sample; (b and c) morphology of rGO-30 and rGO-90 layer, respectively.

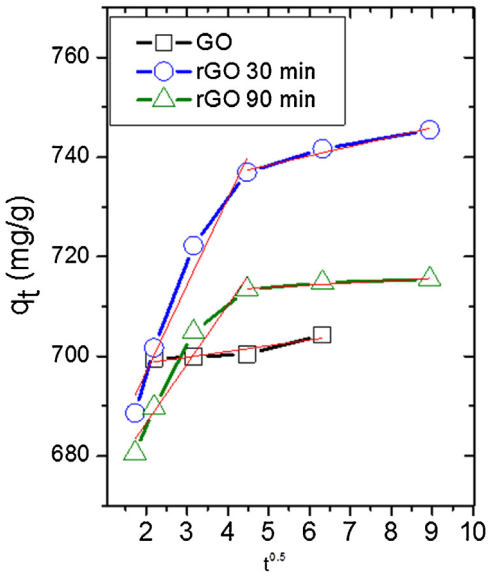


**Fig. 6.** Intra-particle diffusion plot of GO, rGO-30 and rGO-90.

transfer process within a short period of time and that GO does not possess a porous structure, as shown by AFM analysis in Fig. 5.

Therefore, we suggest that the adsorption mechanism for rGO-30 and rGO-90 involves several stages, i.e. instantaneous adsorption of MB on rGO surface, intra-particle diffusion of the dye into the pores and finally the establishment of the equilibrium.

It should be noted that after the adsorption of MB on GO and on rGO sheets, there is still a certain amount of MB in the solution that should be removed by an opportune process. One of the most employed methods is the photocatalytic degradation of dyes with $TiO_2$ powder or $TiO_2$ nanowire/nanotubes membranes [11]. Generally, the UV irradiation of $TiO_2$ generates charge carriers, which can destroy various organic substances. However, one limitation of $TiO_2$ for water treatment is the weak degradation under visible light due to the large band gap (about 3.2 eV) [53]. In order to improve the photocatalytic performance of $TiO_2$, many studies have been conducted doping $TiO_2$ with different elements. Recently, graphene oxide (GO) and other graphene related materials have been employed in this direction. In future experiments we will focus on the fabrication of hybrid composites rGO@$TiO_2$ with the laser reduced GO in order to study the properties of the hybrids towards the photodegradation of the residual MB in solution.

## 4. Conclusions

In summary, in the present work we have illustrated that laser treated graphene oxide shows an excellent adsorption capacity towards methylene blue dye in water. In particular, it was found that controlling different parameters during the laser irradiation time it is possible to obtain GO sheets with different degrees of reduction, which could enhance more or less the removal of MB. We observed that both GO and rGO are excellent adsorbents towards MB and we noticed that rGO-30 has a higher adsorption capacity than GO. The enhancement observed for moderately irradiated GO is mainly due to its different morphology. In particular, it was found that the laser treated GO revealed a discontinuous surface where some holes have been detected contributing to an increase of the available rGO surface area (higher adsorption capacity). In our previous work [50], we reported that upon laser ablation it is possible to obtain sheets of porous graphene in a way similar to the coal gasification mechanism. In particular, $sp^3$ carbon atoms of the GO sheet react with $H_2O$ vapour, originated during the laser irradiation, which lead to the formation of CO and $CO_2$ molecules, which leave behind a distribution of carbon vacancies and creating nanopores.

## Acknowledgements

The authors Paola Russo, Luisa D'Urso, Giuseppe Compagnini acknowledge the project PON R&C 2007–2013 (PON02 00355), funded by Ministero Istruzione Universitàe Ricerca.

## Appendix A. Supplementary data

Supplementary data associated with this article can be found, in the online version, at http://dx.doi.org/10.1016/j.apsusc.2014.12.014.

## References

[1] A. Hu, R. Liang, X. Zhang, S. Kurdi, D. Luong, H. Huang, P. Peng, E. Marzbanrad, K.D. Oakes, Y. Zhou, M.R. Servos, Enhanced photocatalytic degradation of dyes by $TiO_2$ nanobelts with hierarchical structures, J. Photochem. Photobiol. A: Chem. 256 (2013) 7–15.
[2] M.M. Ayad, A.A. El-Nasr, Adsorption of cationic dye (methylene blue) from water using polyaniline nanotubes base, J. Phys. Chem. C 114 (2010) 14377–14383.
[3] A. Mendez, F. Fernandez, G. Gasco, Removal of malachite green using carbon-based adsorbents, Desalination 206 (2007) 147–153.
[4] V.K. Gupta, Suhas, Application of low-cost adsorbents for dye removal – a review, J. Environ. Manage. 90 (2009) 2313–2342.
[5] B.H. Hameed, A.T.M. Din, A.L. Ahmad, Adsorption of methylene blue onto bamboo-based activated carbon: kinetics and equilibrium studies, J. Hazard. Mater. 141 (2007) 819–825.
[6] H. Wang, X. Yuan, G. Zeng, L. Leng, X. Peng, K. Liao, L. Peng, Z. Xiao, Removal of malachite green dye from wastewater by different organic acid-modified natural adsorbent: kinetics, equilibriums, mechanisms, practical application, and disposal of dye-loaded adsorbent, Environ. Sci. Pollut. Res. 1–13 (2014), http://dx.doi.org/10.1007/s11356-014-3025-2.
[7] O.A. Andreo dos Santos, C.Z. Castelli, M.F. Oliveira, A.F. de Almeida Netob, M.G.C. da Silva, Adsorption of synthetic orange dye wastewater in organoclay, Chem. Eng. Trans. 32 (2013) 307–312.
[8] S. Wang, Z.H. Zhu, Characterization and environmental application of an Australian natural zeolite for basic dye removal from aqueous solution, J. Hazard. Mater. 136 (2006) 946–952.
[9] M.S. Sadri, M.R. Alavi Moghaddam, M. Arami, Coagulation/flocculation process for dye removal using sludge from water treatment plant: optimization through response surface methodology, J. Hazard. Mater. 175 (2010) 651–657.
[10] H.T. Gomes, B.F. Machado, A. Ribeiro, I. Moreira, M. Rosário, A.M.T. Silva, J.L. Figueiredo, J.L. Faria, Catalytic properties of carbon materials for wet oxidation of aniline, J. Hazard. Mater. 159 (2008) 420–426.
[11] A. Hu, X. Zhang, K.D. Oakes, P. Peng, Y. Zhou, M. Servos, Hydrothermal growth of free standing $TiO_2$ nanowire membranes for photocatalytic degradation of pharmaceuticals, J. Hazard. Mater. 189 (2011) 278–285.
[12] A. Hu, X. Zhang, D. Luong, K.D. Oakes, M.R. Servos, R. Liang, S. Kurdi, P. Peng, Y. Zhou, Adsorption and photocatalytic degradation kinetics of pharmaceuticals by $TiO_2$ nanowires during water treatment, Waste Biomass Valoriz. 3 (2012) 443–449.
[13] M.N. Chong, B. Jin, C.W.K. Chow, C. Saint, Recent developments in photocatalytic water treatment technology: a review, Water Res. 44 (2010) 2997–3027.
[14] G. McKay, G. Ramprasad, P.P. Mowli, Equilibrium studies for the adsorption of dyestuffs from aqueous solutions by low-cost materials, Water Air Soil Pollut. 29 (1986) 273–283.
[15] Y.C. Sharma, Uma, S.N. Upadhyay, F. Gode, Adsorptive removal of a basic dye from water and wastewater by activated carbon, J. Appl. Sci. Environ. Sanit. 4 (2009) 21–28.
[16] C. Namasivayam, N. Muniasamy, K. Gayathri, M. Rani, K. Ranganathan, Removal of dyes from aqueous solutions by cellulosic waste orange peel, Bioresour. Technol. 57 (1996) 37–43.
[17] D. Mahanta, G. Madras, S. Radhakrishnan, S. Patil, Adsorption and desorption kinetics of anionic dyes on doped polyaniline, J. Phys. Chem. B 113 (2009) 2293–2299.
[18] E.N. El Qada, S.J. Allen, G.M. Walker, Adsorption of methylene blue onto activated carbon produced from steam activated bituminous coal: a study of equilibrium adsorption isotherm, Chem. Eng. J. 124 (2006) 103–110.
[19] M.U. Dural, L. Cavas, S.K. Papageorgiou, F.K. Katsaros, Methylene blue adsorption on activated carbon prepared from *Posidonia oceanica* (L.) dead leaves: kinetics and equilibrium studies, Chem. Eng. J. 168 (2011) 77–85.
[20] B.H. Hameed, A.L. Ahmad, K.N.A. Latiff, Adsorption of basic dye (methylene blue) onto activated carbon prepared from rattan sawdust, Dyes Pigments 75 (2007) 143–149.
[21] N.M. Mahmoodi, Zinc ferrite nanoparticle as a magnetic catalyst: synthesis and dye degradation, Mater. Res. Bull. 48 (2013) 4255–4260.

[22] J. Liu, Z. Gao, H. Han, D. Wu, F. Xu, H. Wang, K. Jiang, Mesoporous $Cu_2O$ submicrospheres, facile synthesis and the selective adsorption properties, Chem. Eng. J. 185–186 (2012) 151–159.
[23] H. Wang, X. Yuan, Y. Wu, H. Huang, X. Peng, G. Zeng, H. Zhong, J. Liang, M. Ren, Graphene-based materials: fabrication, characterization and application for the decontamination of wastewater and waste gas and hydrogen storage/generation, Adv. Colloid Interface Sci. 195–196 (2013) 19–40.
[24] G.K. Ramesha, A.V. Kumara, H.B. Muralidhara, S. Sampath, Graphene and graphene oxide as effective adsorbents toward anionic and cationic dyes, J. Colloid Interface Sci. 361 (2011) 270–277.
[25] M.Z. Iqbal, A.A. Abdala, Thermally reduced graphene: synthesis, characterization and dye removal applications, RSC Adv. 3 (2013) 24455–24464.
[26] N. Cai, P. Larese-Casanova, Sorption of carbamazepine by commercial graphene oxides: a comparative study with granular activated carbon and multiwalled carbon nanotubes, J. Colloid Interface Sci. 426 (2014) 152–161.
[27] K.S. Novoselov, A.K. Geim, S.V. Morozov, D. Jiang, Y. Zhang, S.V. Dubonos, I.V. Grigorieva, A.A. Firsov, Electric field effect in atomically thin carbon films, Science 306 (2004) 666–669.
[28] C.N.R. Rao, A.K. Sood, K.S. Subrahmanyam, A. Govindaraj, Graphene: the new two-dimensional nanomaterial, Angew. Chem. Int. Ed. 48 (2009) 7752.
[29] L. Chen, J. Yang, X. Zeng, L. Zhang, W. Yuan, Adsorption of methylene blue in water by reduced graphene oxide: effect of functional groups, Mater. Express 3 (2013) 281–290.
[30] S.F. Spanò, G. Isgrò, P. Russo, M.E. Fragalà, G. Compagnini, Tunable properties of graphene oxide reduced by laser irradiation, Appl. Phys. A 117 (2014) 19–23.
[31] S. Barcikowski, G. Compagnini, Advanced nanoparticle generation and excitation by lasers in liquids, Phys. Chem. Chem. Phys. 15 (2013) 3022–3026.
[32] G. Compagnini, E. Messina, O. Puglisi, R.S. Cataliotti, V. Nicolosi, Spectroscopic evidence of a core–shell structure in the earlier formation stages of Au–Ag nanoparticles by pulsed laser ablation in water, Chem. Phys. Lett. 457 (2008) 386–390.
[33] P. Liu, H. Cui, C.X. Wang, G.W. Yang, From nanocrystal synthesis to functional nanostructure fabrication: laser ablation in liquid, Phys. Chem. Chem. Phys. 12 (2010) 3942–3952.
[34] C. Nethravathi, M. Rajamathi, Chemically modified graphene sheets produced by the solvothermal reduction of colloidal dispersions of graphite oxide, Carbon 46 (2008) 1994–1998.
[35] Y. Zhou, Q. Bao, L.A.L. Tang, Y. Zhong, K.P. Loh, Hydrothermal dehydration for the "green" reduction of exfoliated graphene oxide to graphene and demonstration of tunable optical limiting properties, Chem. Mater. 21 (2009) 2950–2956.
[36] S. Dubin, S. Gilje, K. Wang, V.C. Tung, K. Cha, A.S. Hall, J. Farrar, R. Varshneya, Y. Yang, R.B. Kaner, A one-step, solvothermal reduction method for producing reduced graphene oxide dispersions in organic solvents, ACS Nano 4 (2010) 3845–3852.
[37] T.H. Han, Y.-K. Huang, A.T.L. Tan, V.P. Dravid, J. Huang, Steam etched porous graphene oxide network for chemical sensing, J. Am. Chem. Soc. 133 (2011) 15264–15267.
[38] S. Stankovich, D.A. Dikin, G.H.B. Dommett, K.M. Kohlhaas, E.J. Zimney, E.A. Stach, R.D. Piner, S.T. Nguyen, R.S. Ruoff, Graphene-based composite materials, Nature 442 (2006) 282–286.
[39] C. Gomez-Navarro, R.T. Weitz, A.M. Bittner, M. Scolari, A. Mews, M. Burghard, K. Kern, Electronic transport properties of individual chemically reduced graphene oxide sheets, Nano Lett. 7 (2007) 3499–3503.
[40] J. Tauc, Optical properties and electronic structure of amorphous Ge and Si, Mater. Res. Bull. 3 (1968) 37–46.
[41] J. Tauc, R. Grigorovici, A. Vancu, Optical properties and electronic structure of amorphous germanium, Phys. Stat. Sol. 15 (1996) 627–637.
[42] G. Eda, Y.-Y. Lin, C. Mattevi, H. Yamaguchi, H.-A. Chen, I.-S. Chen, C.-W. Chen, M. Chhowalla, Blue photoluminescence from chemically derived graphene oxide, Adv. Mater. 22 (2010) 505–509.
[43] P. Russo, G. Compagnini, C. Musumeci, B. Pignataro, Raman monitoring of strain induced effects in mechanically deposited single layer graphene, J. Nanosci. Nanotechnol. 12 (2012) 8755–8758.
[44] G. Sobon, J. Sotor, J. Jagiello, R. Kozinski, M. Zdrojek, M. Holdynski, P. Paletko, J.B. lawski, L. Lipinska, K.M. Abramski, Graphene oxide vs. reduced graphene oxide as saturable absorbers for Er-doped passively mode-locked fiber laser, Opt. Express 20 (2012) 19463–19473.
[45] B. Konkena, S. Vasudevan, Understanding aqueous dispersibility of graphene oxide and reduced graphene oxide through pKa measurements, J. Phys. Chem. Lett. 3 (2012) 867–872.
[46] D. Li, M.B. Muller, S. Gilje, R.B. Kaner, G.G. Wallace, Processable aqueous dispersions of graphene nanosheets, Nat. Nanotechnol. 3 (2008) 101–105.
[47] H. Zhang, X. Han, Z. Yang, J. Zou, H. Tang, Enhanced adsorption of methylene blue on graphene oxide by tuning the oxidation degree of graphene oxide, J. Nanomater. Mol. Nanotechnol. S1003 (2013), http://dx.doi.org/10.4172/2324-8777.S1-003.
[48] H. Qiu, L. Lv, B.-C. Pan, Q.-J. Zhang, W.-M. Zhang, Q.-X. Zhang, Critical review in adsorption kinetic models, J. Zhejiang Univ. Sci. A 10 (2009) 716–724.
[49] C.H. Chia, N.F. Razali, M.S. Sajab, S. Zakaria, N.M. Huang, H.N. Lim, Methylene blue adsorption on graphene oxide, Sains Malaysiana 42 (2013) 819–826.
[50] P. Russo, A. Hu, G. Compagnini, W.W. Duley, N.Y. Zhou, Femtosecond laser ablation of highly oriented pyrolytic graphite: green route for large-scale production of porous graphene and graphene quantum dots, Nanoscale 6 (2014) 2381–2389.
[51] F.-C. Wu, R.-L. Tseng, R.-S. Juang, Initial behavior of intraparticle diffusion model used in the description of adsorption kinetics, Chem. Eng. J. 153 (2009) 1–8.
[52] S.J. Allen, G. McKay, K.Y.H. Khader, Intraparticle diffusion of a basic dye during adsorption onto sphagnum peat, Environ. Pollut. 56 (1989) 39–50.
[53] T. Ohno, T. Tsubota, M. Toyofuku, R. Inaba, Photocatalytic activity of a $TiO_2$ photocatalyst doped with C4+ and S4+ ions having a rutile phase under visible light, Catal. Lett. 98 (2004) 255–258.